Biosensors and Bioelectronics 144 (2019) 111670

Contents lists available at ScienceDirect

Biosensors and Bioelectronics

journal homepage: www.elsevier.com/locate/bios

# A portable immune-thermometer assay based on the photothermal effect of graphene oxides for the rapid detection of *Salmonella typhimurium*

Shuyuan Du[a,1], Ying Wang[a,1], Zhaochen Liu[a], Zhixiang Xu[b,**], Hongyan Zhang[a,*]

[a] Shandong Provincial Key Laboratory of Animal Resistance Biology, Institute of Biomedical Sciences, Key Laboratory of Food Nutrition and Safety of Shandong Normal University, College of Life Science, Shandong Normal University, Jinan, 250014, PR China

[b] College of Food Science and Engineering, Shandong Agricultural University, Tai'an, 271018, PR China

ARTICLE INFO

*Keywords:*
Photothermal effect
Graphene oxides
Immune-thermometer assay
*Salmonella typhimurium*

ABSTRACT

Previously reported photothermal strip test methods generally used a membrane as the antibody carrier and a thermal imaging camera or sensor as detector. To further simplify the detection device, a modified mercury head of the glass thermometer can act as the antibody carrier. Meanwhile, the temperature variation signal (ΔT) generated by the photothermal effect of labeled nanomaterials can be detected by the thermometer directly. Thus, the antibody carrier and detector can be integrated on a portable and cheap thermometer, which greatly simplified the device and detection steps of the photothermal method. The excellent photothermal effect of graphene oxides was used to improve the detection sensitivity. The main parameters of the performance of immune-thermometer assay were optimized and the *Salmonella typhimurium* was chosen as the representative target. Under the optimized conditions, the ΔT and the different number of *Salmonella typhimurium* were plotted to establish the standard curve. The detection limit was estimated to be $10^3$ CFU·mL$^{-1}$. The entire detection operation was consistently finished in 15 min. Overall, the proposed immune-thermometer exhibited good precision, selectivity and acceptable stability. The immune-thermometer assay was also successfully implemented and validated in different foodstuffs, which showed that it can be used as a novel and promising technique for rapid, simple and on-site screening of hazards in food, biological, clinical or environmental samples.

## 1. Introduction

According to the World Health Organization, *Salmonella typhimurium* is one of the major pathogenic bacteria that cause foodborne disease worldwide (Havelaar et al., 2015). Currently, several types of techniques have been established to detect *Salmonella typhimurium*, mainly including traditional methods (e.g., bacterial culture methods) and rapid detection methods (e.g., polymerase chain reaction (PCR) analysis (Jangampalli Adi et al., 2017), enzyme-linked immunosorbent assay (ELISA) technique (Ahari et al., 2017; Jain et al., 2012), loop-mediated isothermal amplification (LAMP) test (Kaur et al., 2018; Park et al., 2017; Seo et al., 2017), and biosensors (Xu et al., 2016; Srisa-Art et al., 2018)). With the improvement of requirements for food safety, the sensitive and rapid detection of *Salmonella typhimurium* remains urgently needed.

A series of highly sensitive and rapid detection methods based on the photothermal effect of nanomaterials have been recently established. Bischof et al. proposed a creative solution based on the photothermal effect of gold nanoparticles (GNPs) to significantly improve the detection sensitivity of the strip method by 32-fold compared to visual detection (Qin et al., 2012). Then, they developed a new validated thermal contrast amplification reader based on GNPs to further improve the detection sensitivity of the strip method in quantitative detection (Wang et al., 2016). Jung et al. developed a convenient and straight forward photothermal biosensor for sensitive detection of C-reactive protein using the photothermal effect of GNPs (Lee et al., 2017). Another temperature sensor was developed for rapid, sensitive and quantitative test strip detection using the photothermal effect of GNPs (Zhang et al., 2019; Jia et al., 2019), which can be used for sensitive, simple, rapid and on-site screening of analytes. To achieve the goal of improving the photothermal contrast of nanomaterials in a detection method, instead of GNPs, we have chosen graphene oxides (GOs) (Zhou

* Corresponding author.
** Corresponding author.
*E-mail addresses:* zhixiangxu@sina.com (Z. Xu), zhanghongyan@sdnu.edu.cn (H. Zhang).
[1] Contributed equally to the work.

https://doi.org/10.1016/j.bios.2019.111670
Received 20 April 2019; Received in revised form 25 August 2019; Accepted 31 August 2019
Available online 06 September 2019
0956-5663/ © 2019 Elsevier B.V. All rights reserved.

et al., 2016; Zhang et al., 2016) and magnetic nanomaterials (Zhang et al., 2018) with excellent photothermal effect and stability (Afkhami et al., 2017; Karami et al., 2019a,b) for the sensitive detection of cancer cells or *Salmonella typhimurium*.

Previously reported test strip methods based on the photothermal effect of nanomaterials all used a membrane as the antibody carrier and a thermal imaging camera or sensor as detector. However, membranes are susceptible to breakage, compression and marking during processing, and also greatly affected by the environmental temperature and relative humidity (Du et al., 2014). In addition, the temperature variation (ΔT) generated by nanomaterials must always be recorded using thermal imaging camera or sensor.

To further simplify the detection device and procedure based on photothermal effect of nanomaterials, a novel portable immune-thermometer assay is developed in this work. A new method is proposed involving the replacement of the membrane by a glass thermometer, which simultaneously serves as carrier material and detector. The motivation for this innovative approach is mainly the unique advantages of glass thermometer, such as direct measurement of temperature, low cost and ease of modification. In addition, the rigid and smooth surface, and the high ionic strength tolerance of the glass thermometer are very useful for the resistance against interference from the environment and sample matrix as well as for the improvement of detection sensitivity and accuracy.

Accordingly, a portable immune-thermometer assay was developed for the sensitive and rapid detection of *Salmonella typhimurium* based on the photothermal effect of GOs. The carrier material and detector were integrated into a common glass thermometer, which is more suitable for field detection due to the simplified detection device and procedures, shorter analysis time and lower cost. The successively washed mercury head part of the glass thermometer was modified with amino groups (Scheme 1, A). Then, to specifically recognize *Salmonella typhimurium*, anti-*Salmonella typhimurium* antibodies were immobilized on the surface of thermometer by covalent bonding as shown in Scheme 1 A. The immune-graphene oxide (GO) nanomaterials were obtained by modification of GOs with anti-*Salmonella typhimurium* antibodies as shown in Scheme 1 B. The principle of the sandwich immunoassay of *Salmonella typhimurium* detection is illustrated in Scheme 1 C. The incubation of the modified mercury head with a solution of analyte and immune-GO complexes is shown in Scheme 1 C. Eventually, under laser irradiation, the ΔT was produced due to the photothermal effect of the immune-GO complexes captured on the mercury head, which can be directly detected by the thermometer. The number of *Salmonella typhimurium* was calculated by the calibration curve of the dependence of ΔT on the number of *Salmonella typhimurium* bacteria.

## 2. Material and methods

### 2.1. Reagents and materials

*Salmonella typhimurium*, *Staphylococcus aureus* and *Escherichia coli* were obtained from the National Center for Medical Culture Collections (Beijing, China). The anti-*Salmonella typhimurium* antibody and fluorescein isothiocyanate (FITC)-IgG were obtained from the Beijing Bioss Biological Technology Co. Ltd. (Beijing, China). Carboxyl graphene oxides (GOs) were obtained from Nanjing Xianfeng Nano Material Technology Co. Ltd. (Nanjing, China). (3-aminopropyl) triethoxysilane (APTES) was purchased from Shanghai Kayon Biological Technology Co. Ltd. (Shanghai, China). Absolute methanol, $H_2O_2$ and $H_2SO_4$ were purchased from Tianjin Fuyu Fine Chemical Co. Ltd (Tianjin, China). Bovine serum albumin (BSA) was purchased from Sigma-Aldrich (Missouri, USA). Milk and grape juice were obtained from a local supermarket (Jinan, China). Deionized water was used in all the experiments. All the reagents used in this work were of analytical grade unless otherwise stated.

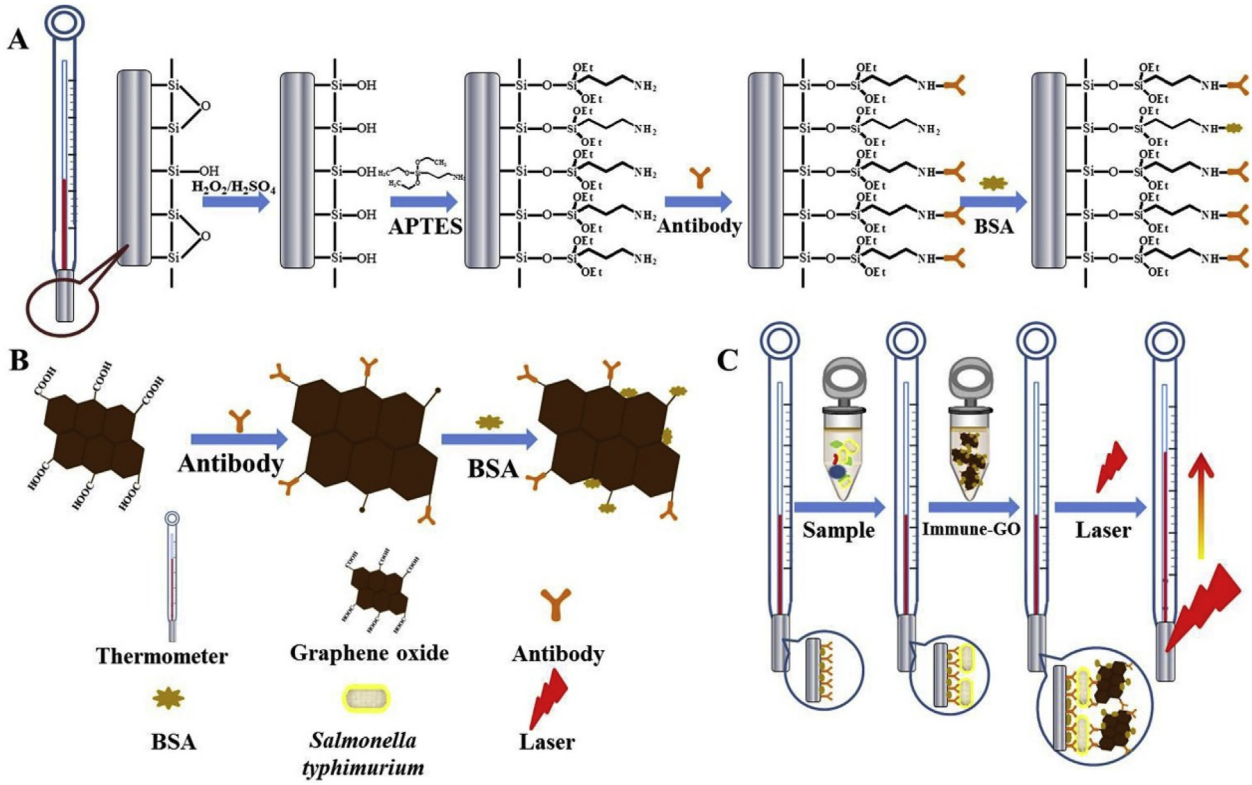


**Scheme 1.** Schematic diagram of immune-thermometer assay used for the rapid detection of *Salmonella typhimurium*. (A) The stepwise procedure of the preparation of the immune-thermometer, (B) Preparation of the immune-GO, (C) Procedure of *Salmonella typhimurium* detection based on the photothermal effect of GOs using immune-thermometer assay.

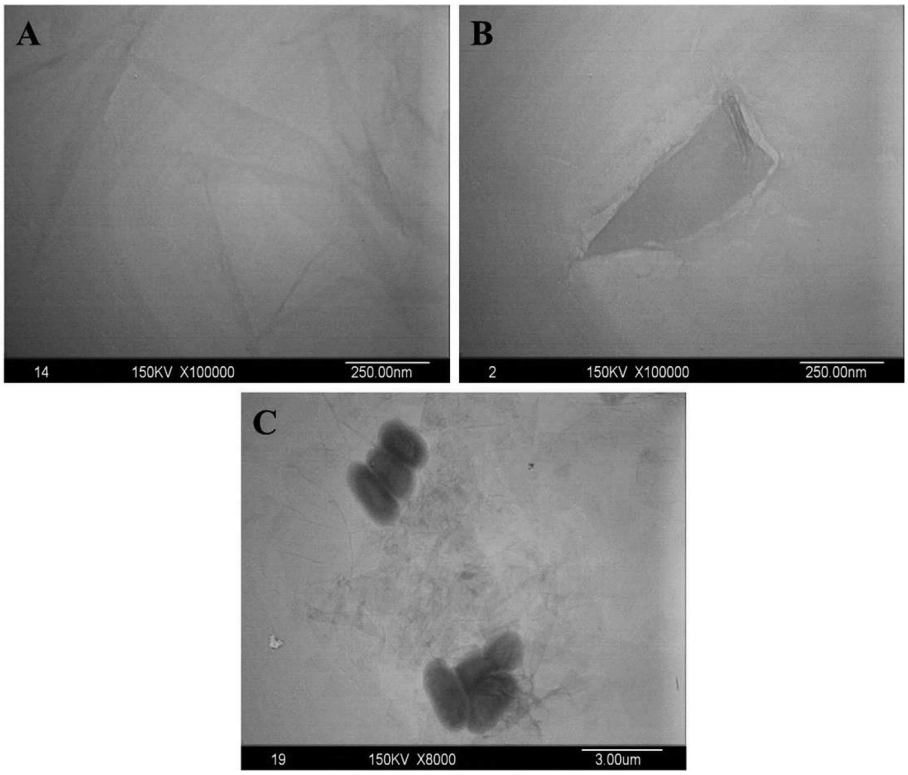


**Fig. 1.** TEM images of the (A) Original GOs, (B) Immune-GO complexes, and (C) *Salmonella typhimurium* recognized by immune-GO complexes.

### 2.2. Apparatus

Thermometers (45 cm, d = 6.2 mm) were purchased from Jinan Chengsen Trade Co. Ltd. (Jinan, China). The near-infrared laser light (808 nm, ADR-1860) was obtained from Shanghai Xilong Optoelectronics Technology Co. Ltd. (Shanghai, China). The transmission electron microscopy (TEM) images were obtained by a JEM-100 CXII electron microscope (JEOL, Tokyo, Japan). The clean bench was obtained from Shandong Boko Bio-Industry Co. Ltd. (Jinan, China). All centrifugations were performed with a MOV-112 purchased from Sanyo Electric International Trading Co. Ltd. (Beijing, China). The shaker incubator was purchased from Shanghai East Instrument Equipment Co. Ltd. (Shanghai, China).

### 2.3. Preparation of the immune-GO complexes

The preparation of the immune-GO complexes was according to the method described in previous work with some modifications (Zhou et al., 2016; Zhang et al., 2018; Karami et al., 2019a,b; Khoshfetrat et al., 2019). Briefly, a 0.5 mL of 20 μg·mL$^{-1}$ solution of anti-*Salmonella typhimurium* antibodies was slowly added to 1 mL of a 200 μg·mL$^{-1}$ GOs solution. After a 2 h reaction at room temperature on a shaker, 0.5 mL of 2% BSA (w/v) was added to the mixture. Then the mixture was incubated for another 2 h at room temperature on a shaker to block the residual surface of the GOs, and stored at 4 °C until further use.

### 2.4. Pretreatment and modification of the mercury head part of the glass thermometer

The mercury head part of the glass thermometer was immersed in a 20 mL "Piranha solution" (30% $H_2O_2$: $H_2SO_4$ = 1:3, below 80 °C), and sonicated for 1 h. Then, it was washed with a large amount of deionized water until the pH of the cleaning solution was neutral, and dried at 65 °C for 2 h.

The mercury head of the glass thermometer should be modified immediately after pretreatment. The pretreated mercury head of the glass thermometer was then immersed in a 10% APTES solution (v/v in absolute methanol) for 2 h at room temperature, which introduces amino groups onto the surface of the thermometer. Absolute methanol was used to wash residual APTES away from the surface of the thermometer. Then the modification reaction was continued for another 30 min in an oven at 50 °C.

### 2.5. Preparation of the immune-thermometer

The modified mercury head of the thermometer was placed vertically in the 3 μg·mL$^{-1}$ anti-*Salmonella typhimurium* antibody solution at 37 °C for 2 h to immobilize the antibodies on the surface of the thermometer. Subsequently, the mercury head was washed with PBS, and then immersed in 2% BSA (w/v) for 2 h at 37 °C to block unspecific sites. Finally, the prepared mercury head of the immune-thermometer was washed with PBS again and stored at 4 °C until use.

### 2.6. Culture and preparation of Salmonella typhimurium

*Salmonella typhimurium* was cultured and prepared according to our previous work with slight modifications (Zhang et al. 2018, 2019). Detailed steps were described in the Electronic Supporting Material (ESM).

### 2.7. Salmonella typhimurium detection procedure

The mercury head of each of the prepared immune-thermometers was incubated in a series of required concentrations of *Salmonella typhimurium* prepared in PBS at 37 °C for 5 min and then immersed in a solution of immune-GO complexes for another 5 min, to capture GOs on the mercury head of the immune-thermometers. Then, the immune-thermometers were washed with PBS. The PBS and samples with no *Salmonella typhimurium* were used as blank and negative controls, respectively. The mercury head of each of the prepared immune-

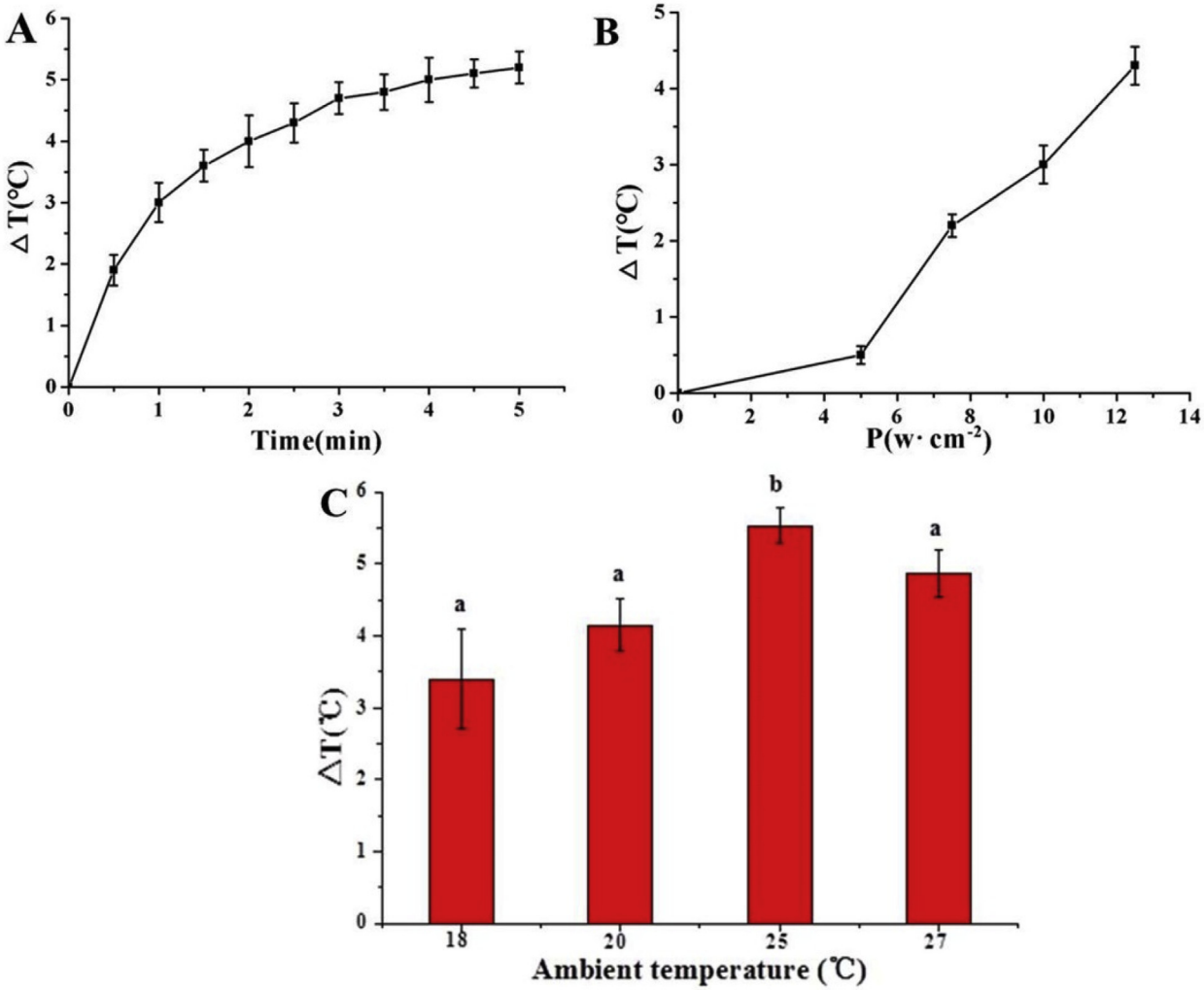


**Fig. 2.** Optimization of the irradiation conditions. (A) Irradiation time, (B) Laser power, (C) Ambient temperature ($p < 0.05$).

thermometer was irradiated with a laser light at 808 nm, which was the most appropriate laser wavelength for GOs as proved by UV–vis spectroscopy. The temperature before and after irradiation was directly recorded with the thermometer. The calibration curve was prepared by plotting the ΔT against the different number of *Salmonella typhimurium* bacteria calculated according to Eq. (1).

$$\Delta T = |\Delta T1 - \Delta T0| \quad (1)$$

Where the ΔT is the temperature variation, the ΔT0 and ΔT1 are the temperature variation before and after irradiation of the blank (unspiked) samples and spiked samples, respectively.

## 3. Results and discussion

### 3.1. Construction and characterization of the immune-GO complexes

The immune-GO complexes were constructed with anti-*Salmonella typhimurium* antibodies and GOs. The original GOs with a diameter of about 200 nm were characterized by TEM, as shown in Fig. 1A. When the GOs were evenly conjugated with anti-*Salmonella typhimurium* antibodies, a significant shadow around the GOs was observed in the TEM image (Fig. 1B), which clearly indicated that the immune-GO complexes had been successfully prepared. The image in Fig. 1C revealed that the *Salmonella typhimurium* bacteria were recognized by the immune-GO complexes and gathered around the nanomaterials.

### 3.2. Optimization of the irradiation conditions of GOs immobilized on the thermometer

The main factors affecting the photothermal effect of the GOs, including the irradiation time, laser power and ambient temperature, were carefully investigated using carboxyl GOs immobilized on the thermometer. The modified mercury head with amino groups was immersed in a solution of 200 $\mu g \cdot mL^{-1}$ carboxyl GOs for 2 h at 25 °C to conjugate the carboxyl GOs on the mercury head. After washing with PBS, the mercury head of the thermometer was irradiated with an 808 nm laser light at 3 $W \cdot cm^{-2}$ for 5 min. The ΔT measurement was directly recorded from the thermometer and the data were analyzed as shown in Fig. 2A. The results revealed that the ΔT increased quickly in the first 3 min, and then leveled off slowly. Stable and high ΔT was obtained at an appropriate irradiation time, which can improve the detection stability, save the detection time and expand the detection range (Jia et al., 2019; Zhou et al., 2016). Accordingly, 3 min was chosen as the optimal irradiation time to achieve rapid detection.

To obtain a suitable ΔT for accurate detection, the laser power should be optimized as shown below. The mercury head with immobilized GOs was irradiated with an 808 nm laser at varying power for 3 min. In Fig. 2B, the ΔT increased significantly with the increase of the laser power from 5 to 12.5 $W \cdot cm^{-2}$. When the laser power was higher than 12.5 $W \cdot cm^{-2}$, the temperature exceeded the thermometer range. Thus, 12.5 $W \cdot cm^{-2}$ was selected as the optimal laser power.

The *t*-test statistical analysis showed that the ΔT at the ambient

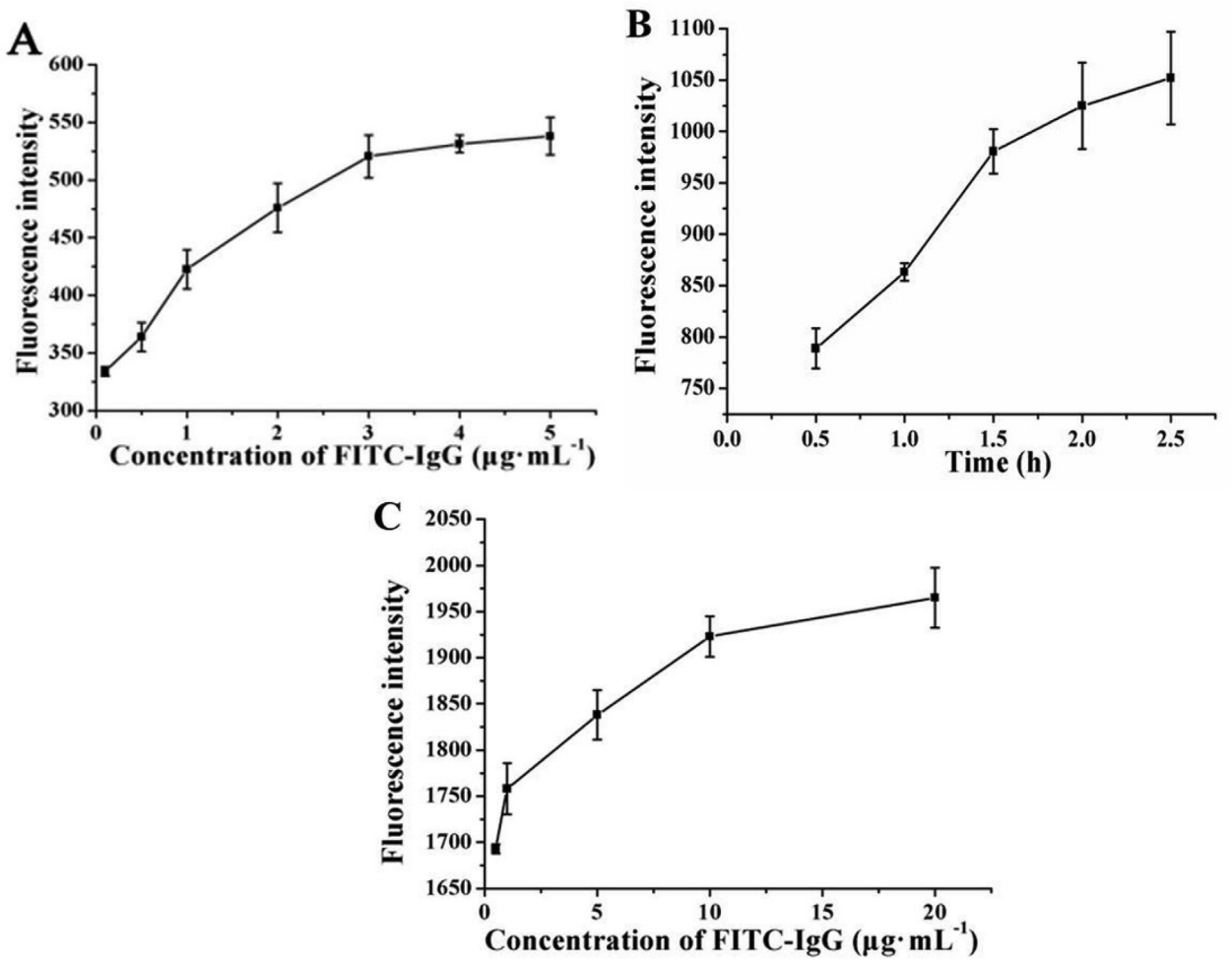


**Fig. 3.** Optimization of the conjugation conditions of the antibody with the mercury head and GOs. (A) Concentration of FITC-IgG immobilized on the mercury head, (B) Incubation time of FITC-IgG with the mercury head, (C) Incubation concentration of FITC-IgG with GOs.

temperature of approximately 25 °C was significantly higher than that of the other temperatures ($p < 0.05$, Fig. 2C), indicating that 25 °C was suitable for subsequent tests. The reason may be that the heat absorption and dissipation on the mercury head of thermometer are balanced (Wang et al., 2018).

### 3.3. Optimization of the immune-thermometer performance

The high sensitivity and low consumption of antibodies are always used as criteria for optimization of the detection method performance. To optimize the amount of antibody conjugated on the mercury head, FITC-IgG, with fluorescent signal produced by FITC, was selected as model protein. The modified mercury head was immersed in a series of FITC-IgG solutions for 2 h at 25 °C to immobilize the FITC-IgG. The mercury head was subsequently washed with PBS, and then immersed in 1 M NaOH to dissociate the FITC-IgG from the thermometer for fluorescence detection. With the increase of the FITC-IgG concentration from 0.1 to 3 μg·mL$^{-1}$ (Fig. 3A), the fluorescence intensity increases rapidly and then reaches a plateau. Therefore, the concentration of antibody used for conjugation on the mercury head was considered to be optimal at 3 μg·mL$^{-1}$. Similarly, when the modified mercury head part was incubated for different time periods from 0.5 to 2 h in a 3 μg·mL$^{-1}$ FITC-IgG solution, the fluorescence intensity increased sharply and then leveled off slowly, as shown in Fig. 3B. This indicated that 2 h was adequate time for conjugating antibodies on the mercury head.

The amount of antibody conjugated on GOs was optimized to improve the detection performance. A series of concentrations of FITC-IgG (0.25 mL) were mixed with 0.5 mL of a 200 μg·mL$^{-1}$ GOs solution. The mixture was allowed to react for 2 h at room temperature on a shaker. The mixture was centrifuged at 7,000 g for 5 min to collect the FITC-IgG immobilized on GOs in the precipitate, and resuspended in 1 mL of PBS for fluorescence intensity detection. Fig. 3C shows that the fluorescence intensity of the resuspended solution increased quickly from 0.5 to 10 μg·mL$^{-1}$ and then increased gradually, indicating that the bonding sites of GOs tended to saturate. Therefore, 10 μg·mL$^{-1}$ was selected as the optimal concentration of antibody for conjugation on the GOs.

### 3.4. Performance evaluation of the immune-thermometer

The sensitivity of the developed immune-thermometer was preliminarily evaluated by detecting *Salmonella typhimurium* in PBS in the concentration range from $10^2$ to $10^9$ CFU·mL$^{-1}$ through verification by the conventional plating assay. The standard curve shown in Fig. 4A, under optimal experimental conditions, was plotted using the ΔT versus the different amounts of *Salmonella typhimurium* bacteria. The limit of detection is defined as 3 times the level of the noise, which was calculated using the ΔT of 10 blank immune-thermometers measured under the optimal experimental conditions. The standard deviation of the mean blank signal was 0.43 °C and was considered as the value of the noise. Therefore, the limit of detection of the immune-thermometer is $10^3$ CFU·mL$^{-1}$. Subsequently, the linearity in the range of $10^3$-$10^9$ CFU·mL$^{-1}$ was obtained between the ΔT and the logarithm of the

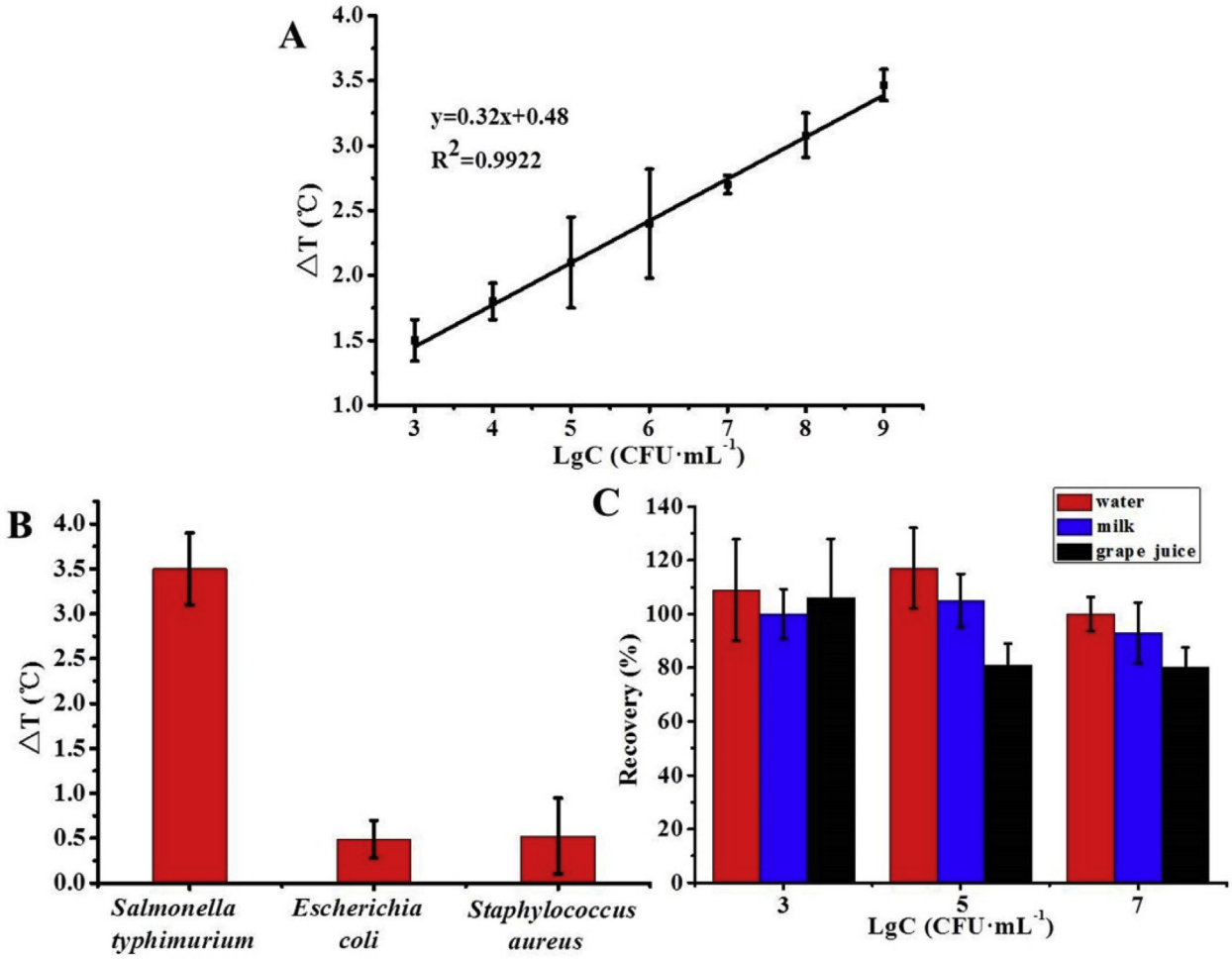


**Fig. 4.** (A) Standard curve of the ΔT and the logarithm of the number of *Salmonella typhimurium* bacteria for the immune-thermometer assay in culture media, (B) Specificity assessment, (C) Detection of *Salmonella typhimurium* spiked in tap water, milk and grape juice.

number of *Salmonella typhimurium* bacteria shown in Fig. 4A. Although the limit of detection of the immune-thermometer was higher than that of the PCR analysis ($1 \times 10^2$ CFU·mL$^{-1}$) (Wang et al., 2017), the whole detection procedure, including sample preparation, was greatly shortened and completed in 15 min. Considering the infective doses of *Salmonella typhimurium* of $10^5$ CFU·mL$^{-1}$ for foodborne disease (Jain et al., 2012), the sensitivity of the immune-thermometer assay is adequate for the effective screening of *Salmonella typhimurium* in foodstuffs.

The repeatability of the developed immune-thermometer assay was evaluated by the coefficient of variation (CV) of the intra-assay and inter-assay. The intra-assay and inter-assay CV were 6.8% and 7.9% respectively, which meet the requirements of a rapid detection method. The stability of the immune-thermometer assay during storage was evaluated with the same batch from zero to 30 day at 4 °C and room temperature. After thirty days of storage at 4 °C and room temperature, the ΔT was exactly the same as that before storage. When placed the immune-thermometer at 37 °C for 2 days, the ΔT retained 80 ± 8.26% (n = 3) compared to the original, which indicated that the immune-thermometer could be stored at 4 °C for at least four months. Such good reproducibility and stability may be due to the excellent stability of the glass thermometer and its effective protection from the environmental conditions including oxygen and humidity. Anti-*Salmonella typhimurium* antibodies were immobilized on the mercury head of the glass thermometer via covalent binding, which is believed to be firmer than the usually exploited electronic attractions and hydrophobic interactions in the test strips (Jain et al., 2012; Wang et al., 2015), and may also improve the repeatability and stability of the immune-thermometer.

### 3.5. Performance assessment of the immune-thermometer assay

*Escherichia coli* and *Staphylococcus aureus* were chosen as non-target bacteria to evaluate the specificity of this immune-thermometer assay. The immune-thermometers were immersed in PBS containing $10^9$ CFU·mL$^{-1}$ of *Salmonella typhimurium*, *Escherichia coli* and *Staphylococcus aureus*, respectively. As shown in Fig. 4B, the ΔT generated by *Salmonella typhimurium* was higher than with non-target bacteria, which was consistent with our previous research (Zhang et al., 2018) and strongly indicated that the specificity of the immune-thermometer based on the photothermal effect of GOs was satisfactory.

Tap water, milk and grape juice were chosen to evaluate the accuracy of the developed immune-thermometer assay, with no *Salmonella typhimurium* after sterilizing at 121 °C for 20 min. Different known amounts of *Salmonella typhimurium* at low, medium and high levels ($10^3$, $10^5$, $10^7$ CFU·mL$^{-1}$) within the linear range of the immune-thermometer assay were spiked into the real samples and prepared as described above and in ESM (Qie et al., 2019). The prepared immune-thermometers were used to capture *Salmonella typhimurium* and determine the ΔT. The data in Fig. 4C showed that the recovery ranged from 100 ± 6.34% (n = 3) to 117 ± 15.02% (n = 3) in tap water, 93 ± 11.42% (n = 3) to 105 ± 10.03% (n = 3) in milk and 80 ± 7.62% (n = 3) to 106 ± 22.03% (n = 3) in grape juice. The results obtained from immune-thermometer assay and bacterial culture method were in good agreement with satisfactory recovery showed in Table S1, suggesting that the tap water, milk and grape juice matrix almost had no influence on the detection. These results indicated that

**Table 1**
The efficiency of different immunoassays for the rapid detection of *Salmonella typhimurium*.

| Methods | Detection time | Matrix | Linear range ($CFU{\cdot}mL^{-1}$) | Detection limit ($CFU{\cdot}mL^{-1}$) | Instrument | References |
|---|---|---|---|---|---|---|
| Lateral flow immunoassay | 10 min | PBST Pure milk | | $1.25\times10^5$ $1.25\times10^6$ | No | Wang et al. (2015) |
| ELISA | 3 h | PBST Pure milk | | $10^4$ $1.44\times10^5$ | Microplate reader | Wang et al. (2015) |
| Surface aminated polycarbonate membrane enhanced-ELISA | 4.5 h | PBS | $10^6$-$10^7$ | $2\times10^3$ | Microplate reader | Jain et al. (2012) |
| Gold nanoparticle-based enzyme-linked antibody-aptamer sandwich assay | 3 h | PBS, milk | $10^3$-$10^8$ | $10^3$ | Microplate reader | Wu et al. (2014) |
| Quartz crystal microbalance (QCM) instrument | 12 min | PBS | 10-$10^3$ | 10-20 | QCMA-1 biosensor system | Salam et al. (2013) |
| Electrochemical immunosensor | 1-2 h | Pure culture, beef and chicken | $10^2$-$10^6$ | $1.04\times10^3$ | IM-6 Impedance Analyzer | Xu et al. (2016) |
| Photothermal effect of magnetic nanomaterials | 1.5 h | PBS, drinking water | 300-$10^3$ | 300 | Thermal sensor, laser | Zhang et al. (2018) |
| Immune-thermometer | 15 min | PBS, tap water, milk and grape juice | $10^3$-$10^9$ | $10^3$ | Laser | This work |

the proposed immune-thermometer was highly accurate (Du et al., 2014) and can be used for the target detection of practical samples.

### 3.6. Comparison with existing Salmonella typhimurium immunoassays

The performance of the developed immune-thermometer assay was also compared to other immunoassays used for detecting *Salmonella typhimurium* summarized in Table 1. Considering the difference in antibodies, samples, instruments and the definition of the detection limit among these techniques, it is very difficult to make an accurate comparison of the sensitivity. The detection limit of the immune-thermometer was higher than that of the method used in our previous work (Zhang et al., 2018) and the quartz crystal microbalance (Salam et al., 2013), and similar to that of the surface aminated polycarbonate membrane enhanced-ELISA (Jain et al., 2012) technique, gold nanoparticle-based enzyme-linked antibody-aptamer sandwich assay (Wu et al., 2014) and electrochemical immunosensor (Xu et al., 2016). Furthermore, this method with simple swift quantitative detection, no required instrumentation and excellent dynamic range indicated that the immune-thermometer is an effective tool for screening *Salmonella typhimurium* in foodstuffs. Moreover, the glass thermometer integrates the carrier materials and detector, which decreases the cost and reduces the technical requirements of the testing personnel. Besides, the immune-thermometer with unique advantages like high rigidity and ionic strength tolerance is very amenable to regeneration by dissociation, and will be further investigated in the near future. However, the length of glass thermometer needs to be shortened for more portable and the fragility of glass thermometer also needs to be further improved.

## 4. Conclusion

A novel rapid immune-thermometer assay based on the photothermal effect of GOs was designed and prepared for the rapid and sensitive detection of *Salmonella typhimurium*. The glass thermometer integrated the carrier materials and detector and dramatically simplified the detection device and procedure, which makes it more suitable for field detection with simple measurement steps and reduction of the cost. With *Salmonella typhimurium* as the target, the immune-thermometer assay was developed and its efficiency was comprehensibly evaluated and confirmed. This rapid detection method has the potential for application in on-site screening of foodborne pathogens and hazard factors in food samples. Many new types of nanomaterials with more excellent photothermal effect will be chosen to improve the detection sensitivity of the immune-thermometer assay. Furthermore, the complicated operation steps in regeneration of immune-thermometer assay as well as the portability of glass thermometer need to be further improved in practical application.

## CRediT authorship contribution statement

**Shuyuan Du:** Conceptualization, Methodology, Formal analysis, Writing - original draft, Writing - review & editing. **Ying Wang:** Validation, Formal analysis, Investigation, Writing - original draft. **Zhaochen Liu:** Validation, Formal analysis, Investigation. **Zhixiang Xu:** Resources, Writing - review & editing, Supervision. **Hongyan Zhang:** Conceptualization, Methodology, Resources, Writing - review & editing, Supervision, Project administration.

## Declaration of competing interest

The authors declare that they have no known competing financial interests or personal relationships that could have appeared to influence the work reported in this paper.

## Acknowledgements

This work was supported by the National Natural Science Foundation of China (31871874), the Natural Science Foundation of Shandong Province (ZR2017BCE019), and the China Postdoctoral Science Foundation (2016M602183).

## Appendix A. Supplementary data

Supplementary data to this article can be found online at https://doi.org/10.1016/j.bios.2019.111670.

## References

Afkhami, A., Hashemi, P., Bagheri, H., Salimian, J., Ahmadi, A., Madrakian, T., 2017. Biosens. Bioelectron. 93, 124–131.
Ahari, H., Kakoolaki, S., Anvar, S.A.A., 2017. Int. J. Environ. Sci. Technol. 399, 1–6.
Du, S., Lin, H., Sui, J., Wang, X., Cao, L., 2014. Anal. Bioanal. Chem. 406, 6637–6646.
Havelaar, A.H., Kirk, M.D., Torgerson, P.R., Gibb, H.J., Hald, T., Lake, R.J., Praet, N., Bellinger, D.C., De Silva, N.R., Gargouri, N., Speybroeck, N., Cawthorne, A., Mathers, C., Stein, C., Angulo, F.J., Devleesschauwer, B., 2015. PLoS Med. 12, e1001923.
Jain, S., Chattopadhyay, S., Jackeray, R., Abid, C.K., Kohli, G.S., Singh, H., 2012. Biosens. Bioelectron. 31, 37–43.
Jangampalli Adi, P., Naidu, J.R., Matcha, B., 2017. Microb. Pathog. 110, 50–55.
Jia, M., Liu, J., Zhang, J., Zhang, H., 2019. Analyst 144, 573–578.
Kaur, A., Das, R., Nigam, M.R., Elangovan, R., Pandya, D., Jha, S., Kalyanasundaram, D., 2018. Indian J. Microbiol. 58, 381–392.
Karami, P., Bagheri, H., Johari-Ahar, M., Khoshsafar, H., Arduini, F., Afkhami, A., 2019a. Talanta 111–122 2012.
Karami, P., Khoshsafar, H., Johari-Ahar, M., Arduini, F., Afkhami, A., Bagheri, H., 2019b. Spectrochim. Acta 222, 117218.
Khoshfetrat, S.M., Khoshsafar, H., Afkhami, A., Mehrgardi, M.A., Bagheri, H., 2019. Anal. Chem. 91, 6383–6390.
Lee, S.H., Choi, S., Kwon, K., Bae, N.-H., Kwak, B.S., Cho, W.C., Lee, S.J., Jung, H.-I., 2017. Sens. Actuators B Chem. 246, 471–476.
Park, B.H., Oh, S.J., Jung, J.H., Choi, G., Seo, J.H., Kim, D.H., Lee, E.Y., Seo, T.S., 2017. Biosens. Bioelectron. 91, 334–340.
Qie, Z., Liu, Q., Yan, W., Gao, Z., Meng, W., Xiao, R., Wang, S., 2019. Anal. Chem. 91, 9530–9537.
Qin, Z., Chan, W.C.W., Boulware, D.R., Akkin, T., Butler, E.K., Bischof, J.C., 2012. Angew. Chem. Int. Ed. 51, 4358–4361.
Salam, F., Uludag, Y., Tothill, I.E., 2013. Talanta 115, 761–767.
Seo, J.H., Park, B.H., Oh, S.J., Choi, G., Kim, D.H., Lee, E.Y., Seo, T.S., 2017. Sens. Actuators B Chem. 246, 146–153.
Srisa-Art, M., Boehle, K.E., Geiss, B.J., Henry, C.S., 2018. Anal. Chem. 90, 1035–1043.
Wang, D., Dong, H., Li, M., Cao, Y., Yang, F., Zhang, K., Dai, W., Wang, C., Zhang, X., 2018. ACS Nano 26, 5241–5252.
Wang, M., Yang, J., Gai, Z., Huo, S., Zhu, J., Li, J., Wang, R., Xing, S., Shi, G., Shi, F., 2017. Int. J. Food Microbiol. 266, 251–256.
Wang, W., Liu, L., Song, S., Tang, L., Kuang, H., Xu, C., 2015. Sensors 15, 5281–5292.
Wang, Y., Qin, Z., Boulware, D.R., Pritt, B.S., Sloan, L.M., González, I.J., Bell, D., Rees-Channer, R.R., Chiodini, P., Chan, W.C.W., Bischof, J.C., 2016. Anal. Chem. 88, 11774–11782.
Wu, W., Li, J., Pan, D., Li, J., Song, S., Rong, M., Li, Z., Gao, J., Lu, J., 2014. ACS Appl. Mater. Interfaces 6, 16974–16981.
Xu, M., Wang, R., Li, Y., 2016. Talanta 148, 200–208.
Zhang, D., Du, S., Su, S., Wang, Y., Zhang, H., 2019. Biosens. Bioelectron. 123, 19–24.
Zhang, H., Zhang, Z., Wang, Y., Wu, C., Li, Q., Tang, B., 2016. ACS Appl. Mater. Interfaces 8, 29933–29938.
Zhang, Z., Wang, Q., Han, L., Du, S., Yu, H., Zhang, H., 2018. Sens. Actuators B Chem. 268, 188–194.
Zhou, J., Zheng, Y., Liu, J., Bing, X., Hua, J., Zhang, H., 2016. J. Pharm. Biomed. Anal. 117, 333–337.